JOURNAL OF AIRCRAFT
Vol. 42, No. 4, July–August 2005

Design and Evaluation of Composite Fuselage Panels Subjected to Combined Loading Conditions

Damodar R. Ambur* and Marshall Rouse†
NASA Langley Research Center, Hampton, Virginia 23681-001

Methodologies used in industry for designing transport aircraft composite fuselage structures are discussed. Several aspects of the design methodologies are based on assumptions from metallic fuselage technology, which requires that full-scale structures be tested with the actual loading conditions to validate the designs. Composite panels that represent crown and side regions of a fuselage structure are designed by the use of this approach and tested in biaxial tension. Descriptions of the state-of-the-art test facilities used for this structural evaluation are presented. These facilities include a pressure-box test machine and a D-box test fixture in a combined loads test machine, which are part of a combined loads test system. Nonlinear analysis results for a reference shell and a stiffened composite panel tested in the pressure-box test machine with and without damage are presented. The analytical and test results are compared to assess the ability of the pressure-box test machine to simulate a shell stress state with and without damage. A combined loads test machine for testing aircraft primary structures is described. This test machine includes a D-box test fixture to accommodate curved stiffened panels, and the design features of this test fixture are presented. Finite element analysis results for a curved panel to be tested in the D-box test fixture are also discussed.

Introduction

THE potential for cost and weight reductions still exists for aircraft structures made of polymeric composite materials, despite recent material and manufacturing advances for metallic materials. This potential can be realized in aircraft fuselage structures by judicial integration of materials, structural design and analysis practices, and manufacturing processes. Assessment of the advantages of the use of different materials and material forms and understanding the response of aircraft structures subjected to combined loading conditions are important aspects of the design of aircraft structures. Current composite structural designs are based on metallic structural experience-based approximations for design loads and individual panel analysis and sizing techniques. Such a metals-based design approach can result in a composite structural design with inadequate margins of safety. Structures are analyzed at the local level to satisfy damage tolerance and durability requirements. Existing tension-fracture and impact damage data from flat laminates are currently used to design stiffened-skin and sandwich shell structures, which could result in very conservative structural designs. A very limited amount of information currently exists for curved stiffened panels subjected to combined loading conditions to support the design of composite fuselage structures with large-size damage. Because composite structures have more material design variables than metallic structures, better design and analysis approaches are necessary to design efficient structures and to assess properly the advantages of the use of composite structures to replace metallic structures. Tests of composite structures are likely to be an integral part of the development and validation of designs for composite structures in the future.

Analytical and experimental work on composite fuselage crown and side panels is currently being conducted at NASA Langley Research Center to help study issues related to the nonlinear response, tensile fracture, damage tolerance, and residual strength of composite structures. New facilities are being developed to test new structural concepts subjected to combined internal pressure and mechanical loads. A pressure-box test machine and a combined loads test system with a D-box test fixture have been designed and fabricated to test structural panels with boundary conditions that simulate the actual stress states for panels in a fuselage shell structure. These new test facilities are designed to test damaged and undamaged panels subjected to actual flight load conditions.

The present paper presents an integrated approach for the design of structures to satisfy performance, producibility, and cost requirements. The paper describes the pressure-box test machine and the D-box test fixture for a combined loads test machine. It also describes how these new facilities are being used to simulate the actual stress states in a fuselage shell. Analytical and experimental results are presented and compared for two composite curved panels tested in the pressure-box test machine. Analytical results are also presented that relate test results for panels subjected to combined loads to fuselage shell results. The need to include nonlinear effects in the analysis and the design of pressurized composite structures are also discussed.

Design Methods for Fuselage Structure

The current approach for the design of fuselage shell structures is based on the design of individual panels based on the fuselage load distribution and manufacturing considerations. A fuselage barrel section divided into three different panels is shown in Fig. 1. The panels represent the crown, side, and keel panels for the section. Each panel is further subdivided into smaller-sized panels with approximately uniform stress states. They are analyzed and sized to satisfy stability and strength requirements. Because manufacturing procedures and cost are important elements in the development of a transport composite fuselage, an integrated design approach is used that includes all structures and manufacturing disciplines in the design process for sizing the smaller-sized panels.

This integrated design approach includes the traditional structural design, structural analysis, weights, cost, and manufacturing disciplines. The internal load distribution is determined from a finite element analysis model. Manufacturing processes that are appropriate for the structural concepts and material forms are selected to assure cost-effective fabrication of the structural parts, and the material strength, stiffness properties, and design and manufacturing cost centers are identified. Structural design constraints including

Presented as Paper 97-1303 at the AIAA/ASME/ASCE/AHS/ASC 38th Structures, Structural Dynamics, and Materials Conference, Kissimee, FL, 7–10 April 1997; received 3 March 2002; revision received 1 December 2002; accepted for publication 12 February 2003.

*Head, Mechanics and Durability Branch. Associate Fellow AIAA.
†Senior Aerospace Engineer, Mechanics and Durability Branch. Senior Member AIAA.

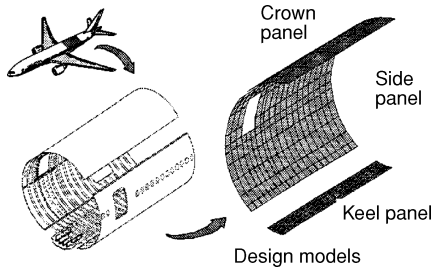

Fig. 1 Hierarchy of design models.

stability, strength, skin-to-stringer and skin-to-frame stiffness ratios, minimum skin gauge, stringer spacing, ply layup, stringer height, minimum stringer flange width, stringer web angle, etc., are used for the structural analysis and sizing of the smaller-size panels. Additional constraints are imposed for damage tolerance and durability. A panel blending algorithm is used to optimize and assemble all of the smaller-size panels into a larger panel design such that structural continuity is maintained for the skin, stringers, and frames. Design rules based on empirical and semi-empirical data are defined for blending the designs of several skin laminates, stringers, and frames. The designer identifies one or more subdivided panels with regions of high stress concentrations to assure that the blending variables in noncritical areas of the panel are controlled by those for the critical areas, and a preliminary design for the fuselage shell is generated. Because the structural definition is usually completed to the 70–80% level of the final structural configuration during the preliminary design phase, it is important to use accurate structural analysis methods for this part of the design process. Finite element analyses are performed by the use of the preliminary design as a starting point to arrive at a final design.

Evaluation of Fuselage Panels Subjected to Combined Loads

A common approach for the study of the damage tolerance characteristics of pressure-loaded stiffened panels is to test flat panels with combinations of tension and compression loads in the longitudinal and lateral directions. These tests are relatively easy to perform, but the data generated from such tests are not directly applicable to the design of pressure-loaded curved panels because the bending gradients in the skin and the resulting nonlinear effects are not represented by the simpler tests. The best approach for determination of the effect of these nonlinear response phenomena is to perform tests on a cylindrical shell to generate the required structural response information. Another approach for tests of curved panels with combined compression, internal pressure, and inplane shear loading conditions is to mount a test panel in a cylindrical shell test fixture that has a cutout to accommodate the test panel. The panel is then subjected to the intended combined loading conditions by loading the cylindrical shell test fixture. The correct boundary conditions can be imposed on the test specimen more readily by the use of this approach. This approach is useful unless it is necessary to test panels with different radii than the radius of the cylindrical shell test fixture. To avoid the expense of building a series of cylindrical shell test fixtures with different radii, a pressure-box test machine and a D-box test fixture have been developed to test curved stiffened panels of different radii and frame spacings. The pressure-box test machine is used to test curved stiffened panels subjected to internal pressure and biaxial tension loading conditions, and the D-box test fixture has been developed to test curved stiffened panels subjected to combined internal pressure, compression, and shear loads compression by the use of a combined loads test machine. Analytical and test results for two typical fuselage panels tested in the pressure-box test machine, and analytical results that supported the design and development of the D-box test fixture, are presented in the next section.

Biaxial Tension Loading Conditions

A photograph of the pressure-box test machine used to test curved stiffened panels subjected to internal pressure and biaxial tension loads is shown in Fig. 2. This pressure-box test machine was designed to ensure that the appropriate boundary conditions are imposed on a pressurized curved panel to develop a stress state in the panel that is representative of a fuselage shell. This design requirement is particularly important when failure of curved panels is investigated and for damage propagation studies. For both the undamaged and damaged states of the panels investigated with this test machine, it is possible to develop the proper stress magnitudes and gradients in a curved panel that are representative of the stress state in a shell with the corresponding loading conditions. A detailed description of this test machine is presented in Ref. 1.

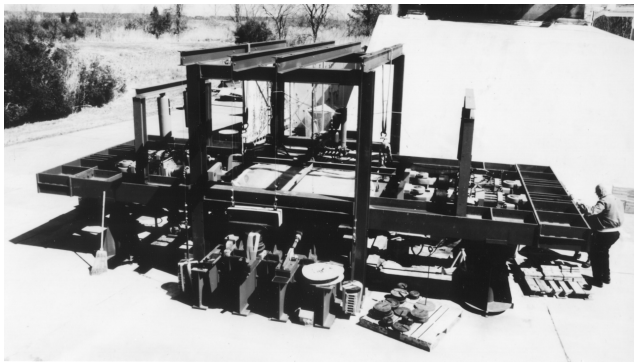

Fig. 2 Pressure-box test machine.

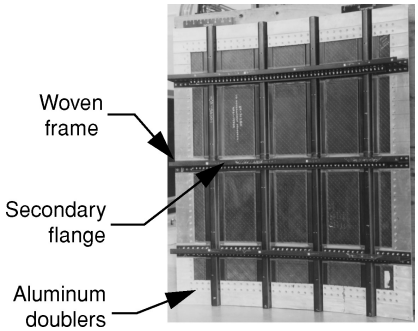

Fig. 3 Composite fuselage panel.

Fuselage Crown Panel Evaluation

A stiffened graphite–epoxy fuselage crown panel shown in Fig. 3 was tested in the pressure-box test machine to study its response characteristics. The panel has a 122-in. (3.10 m) radius, a 72-in. (1.83 m) length, and a 63-in. arc width. The material type and material properties for this panel are presented in Ref. 1. The panel skin is tow-placed by the use of a fiberglass–graphite–epoxy hybrid material system to improve the damage tolerance characteristics of the panel. The panel frames are made of triaxially braided graphite fiber, preform impregnated with an epoxy resin, and cured by the use of a resin transfer molding (RTM) process. The stringers pass through cutouts machined into the frames, and no clips are used to attach the stringers to the frames. This design detail reduces the structural part count and the cost associated with panel fabrication.

The crown panel was analyzed by the use of a nonlinear finite element code to determine the hoop-load reaction forces needed for the panel to simulate the stress state in the corresponding shell and to provide analysis results to correlate with the test data for the damaged and undamaged test specimen. The hoop-load reaction forces are generated by adjustment of a series of turnbuckles that attach the skin and the frames to the load reaction frame of the test machine. Finite element models for the cylindrical shell and the test panel in the pressure-box test machine were generated with PATRAN (Ref. 2). Nonlinear structural analyses for both the shell and the test panel were performed with STAGS (Ref. 3).

The finite element models for the test panel and the shell are shown in Fig. 4. The one-quarter model for the panel shown in

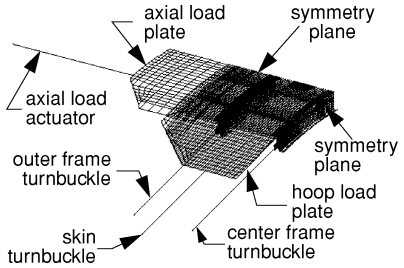

a) Curved panel in the pressure-box test machine

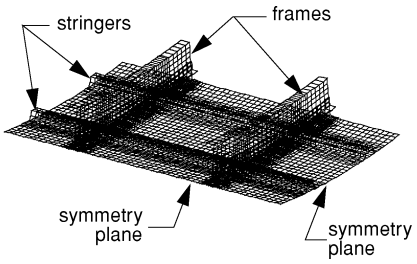

b) Cylindrical shell

Fig. 4 Finite element models.

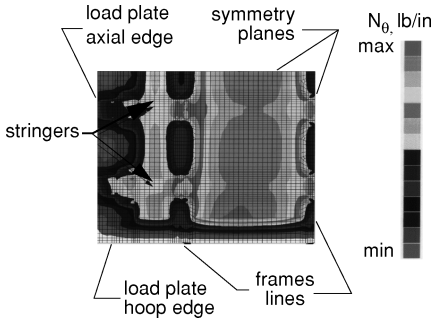

a) Curved panel in the pressure-box test machine

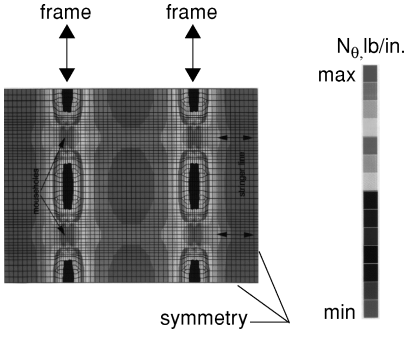

b) Cylindrical shell

Fig. 5 Typical hoop stress contour results.

Fig. 4a has approximately 10,000 shell, rod, and beam elements and 62,000 degrees of freedom. The load introduction structure, the turnbuckles, and actuator rods for the axial hydraulic jacks are modeled to account for rigid-body displacements and flexibilities at the panel boundaries. The shell reference model is shown in Fig. 4b. The model has symmetry boundary conditions; 16,686 shell and beam elements; and 100,000 degrees of freedom. Analytical hoop stress resultant results for the test panel subjected to 18 psi of internal pressure are compared with analytical shell results in Fig. 5. The nonlinear analysis results for the panel with the turnbuckle loads adjusted to the required magnitude indicate that the boundaries influence the stress state in the load introduction region, but the stress states in the interior of the panel compare very well with the stress states for the shell structure. The hoop stress gradients for the reference shell and the panel in the pressure box with a 22-in. long notch are compared in Fig. 6. The location of the maximum value for the

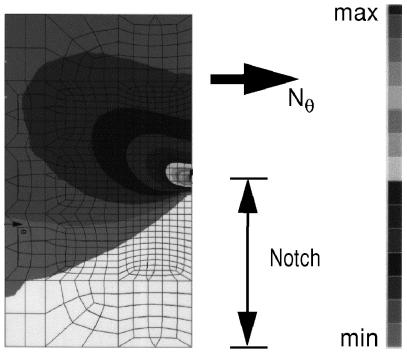

a) Curved panel in the pressure-box test machine

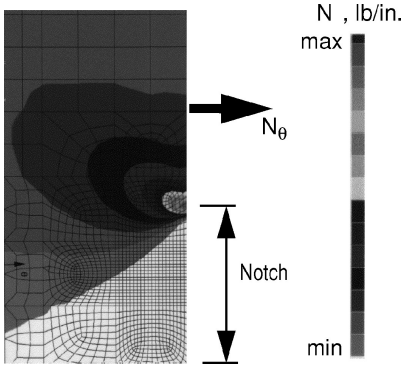

b) Cylindrical shell

Fig. 6 Typical hoop stress contour results at notch tip.

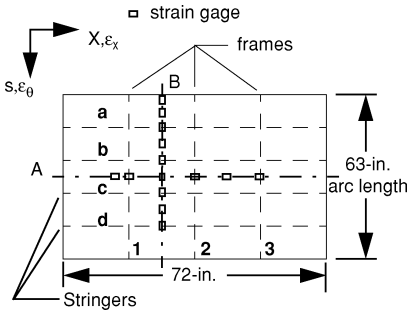

a) Strain-gage locations

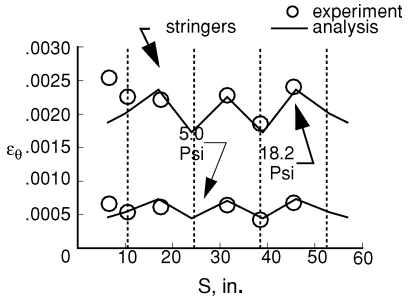

b) Hoop strains along line B

Fig. 7 Comparison of experimental and analytical hoop strain results.

hoop stress resultant for both models is at the notch tip. The magnitudes for the hoop stress resultants also compare well with one another in the interior of the panel, but there are some differences in the results due to the load introduction effects at the boundaries of the curved panel. The undamaged test panel was subjected to an internal pressure of 18.2 psi and an axial load of 1110 lb/in. This pressure value corresponds to twice the operating pressure, the design limit load condition for the fuselage structure. Analytical and experimental hoop strain results are compared for the panel in Fig. 7, and the strain-gauge locations are defined in Fig. 7. The results correlate very well for the 5- and 18-psi internal pressure load conditions

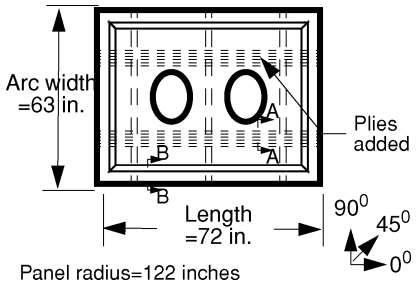

a) Plan view of panel design

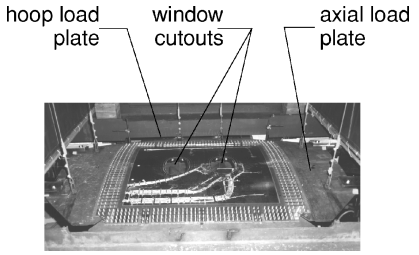

b) Photograph of sandwich panel in pressure-box test machine

Fig. 8 Details for the sandwich panel.

shown in Fig. 7. After the undamaged panel test was completed, a notch was cut into the panel skin to study the damage tolerance characteristics of the panel. Damage growth initiated at the notch tips for an internal pressure of 6.3 psi, and grew along a curved trajectory at approximately 11.2 psi of internal pressure. The details of the experimental results for the damaged panel are presented in Ref. 1. These results illustrate that the pressure-box test machine can be used to simulate a shell stress state in a test panel. The test panel exceeded its design requirements for the design burst pressure condition (twice the design limit load condition) in the undamaged state and satisfied the design limit load condition with damage.

Sandwich Fuselage Side Panel Evaluation

Sandwich fuselage side panels with window cutouts have also been evaluated with the pressure-box test machine. One of the sandwich panels is shown in Fig. 8a and has three frames, a 122-in. radius, a 72-in. length, and a 63-in. arc width. The panel has two window cutouts located midway between the center frame and each of the outer frames. The elliptical window cutouts are 19.92 in. long in the fuselage circumferential direction and 15.30 in. long in the fuselage longitudinal direction. The sandwich panel facesheets were fabricated from the Hercules, Inc. AS4-8552 graphite–epoxy material system, and the core is a Korex honeycomb core material. The facesheets were made from tow-placed material for the inner plies and fabric material for the outer plies. The fuselage frames and window frames were fabricated from fiber preforms consisting of triaxially braided AS4 graphite fibers impregnated with PR500 epoxy resin and cured by the use of an RTM process. The sandwich skin and the three precured frames were cocured in a single cure stage. Typical material properties for the tow-placed, fabric, and triaxially braided AS4-8552 and AS4-PR500 graphite–epoxy material systems are presented in Table 1. A photograph of the finished test panel assembled in the pressure-box test machine is shown in Fig. 8b. One of the objectives of this effort was to determine whether the structure designed with a three-frame configuration could be used with an increased frame spacing to demonstrate additional potential for aircraft structural weight reductions. A two-frame panel configuration was developed from the tested three-frame panel by removal of its center frame.

A finite element model of the sandwich panel in the pressure-box test machine is shown in Fig. 9. The sandwich panel is modeled by the use of the ABAQUS finite element program[4] with four-node isoparametric elements for the face sheets and three eight-node solid elements through the thickness to represent the honeycomb core. The circumferential frames and the window frames are also modeled

Table 1 Typical material properties for graphite-epoxy materials used to manufacture the sandwich fuselage panel

Property	Tow AS4/8552	Fabric AS4/8552	Triaxial braid AS4/PR500	Korex core
Longitudinal modulus, E_1, 10^6 psi	18.30	9.20	7050	0.00001
Transverse modulus, E_2, 10^6 psi	1.36	9.20	7.50	0.00001
Lateral modulus, E_3, 10^6 psi	1.36	1.30	——	0.0340
In-plane shear modulus, G_{12}, 10^6 psi	0.76	0.72	0.57	0.00001
Transverse shear modulus, G_{23}, 10^6 psi	0.52	0.50	0.40	0.0136
Transverse shear modulus, G_{13}, 10^6 psi	0.76	0.50	0.57	0.0326
Major Poisson's ratio, ν_{12}	0.32	0.04	0.29	0.30

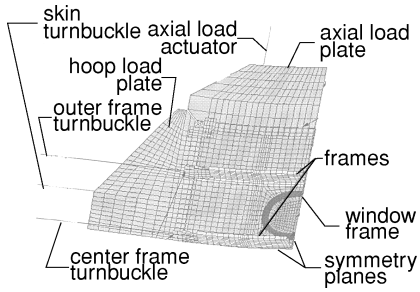

Fig. 9 Finite element model of the sandwich panel.

with the four-node shell elements. The window glazing is also modeled with shell elements. The hoop and axial load introduction plates are modeled with shell elements. Symmetry boundary conditions are assumed at the axial and hoop centerlines, which allows one-quarter of the structure to be modeled and analyzed. The one-quarter model of the test panel in the pressure box has a total of 5343 elements and approximately 26,650 degrees of freedom. This test panel was evaluated in the three- and two-frame configurations for two combined loading conditions: an 18.2-psi burst-pressure condition with 1110 lb/in. of axial tension and a 13.65-psi design ultimate-pressure condition with 2450 lb/in. of axial tension. Finally, the panel with the two-frame configuration was damaged with a cut along the panel hoop direction at the window cutout and tested to the design limit load condition of 8.85 psi of internal pressure and 1630 lb/in. of axial tension.

The analytical hoop and axial strain results for the panel with three frames subjected to the design ultimate loading condition are presented in Fig. 10. The design ultimate loading condition includes 13.65 psi of internal pressure and 2450 lb/in. of axial tension. This loading condition causes high tensile forces in both the panel axial and hoop directions. The stress concentration factors are 2.88 and 2.05 for the hoop and axial stresses, respectively, at the edge of the cutout. The trends of the experimental results agree very well with the finite element analysis results. The experimentally measured strains on the panel outer surface in the hoop direction vary from 1150 μin./in. to -900 μin./in. The finite element analysis results vary from 937 μin./in. to -949 μin./in. The measured strains in the axial direction vary from 4000 μin./in. to -775 μin./in., and the corresponding results from the finite element analysis vary from 3540 μin./in. to -815 μin./in.

The next set of loading conditions imposed on the panel with the center frame removed include 13.65 psi of internal pressure and 2450 lb/in. of axial tension load. The panel outer surface hoop and axial strain results from the finite element analysis for this loading condition are very similar to the results presented in Fig. 10 with the center frame loads redistributing in the sandwich skin. The experimental strain results for the two-frame panel are compared with the three-frame panel results in Fig. 11. Strain-gauge locations around the panel cutout are illustrated in Fig. 11a. The maximum

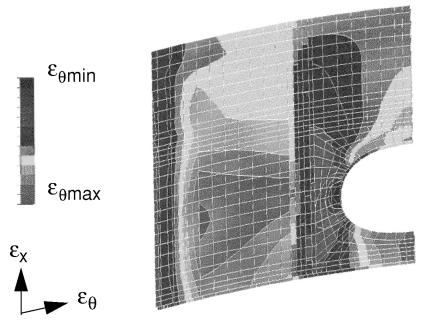

a) Hoop strain contour

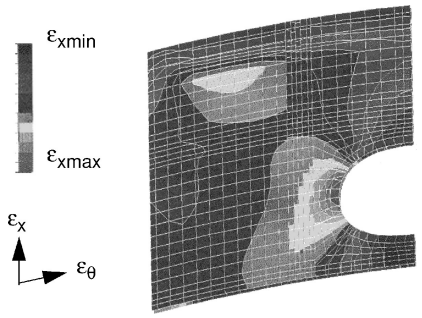

b) Axial strain contour

Fig. 10 Finite element analysis results for strain contours on the panel outer surface for a combined 13.65 psi internal pressure and 2450 lb/in. axial loading condition.

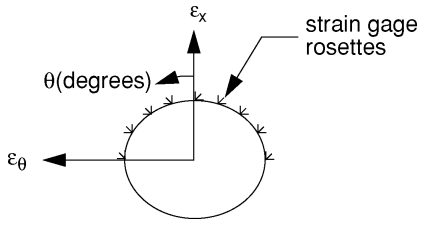

a) Strain gauge locations on the cutout edge

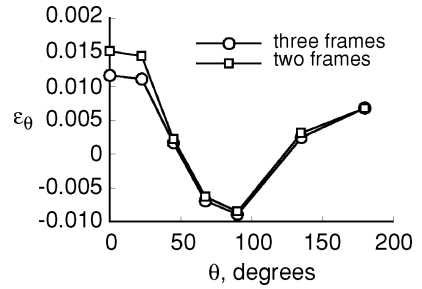

b) Hoop strain

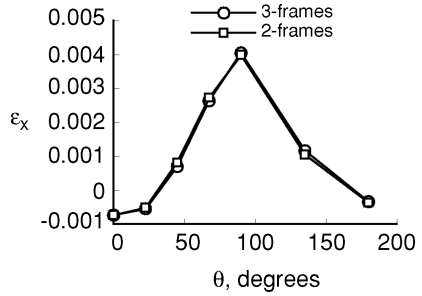

c) Axial strain

Fig. 11 Experimental strain results on the two-frame panel outer surface for a combined 13.65 psi internal pressure and 2450 lb/in. axial loading condition.

axial strain results at the cutout for the two-frame panel vary from -850 μin./in. to 4000 μin./in. compared to the analytical results, which vary from -540 μin./in. to 3860 μin./in. These strain magnitudes are comparable to the axial strains for the three-frame panel for the same load condition.

This configuration was also tested with damage. A maximum value for the axial strain of the undamaged test panel occurs at the edge of the elliptical cutout at its major axis. The magnitude of this strain is 3860 μin./in. for 13.65 psi of internal pressure and 2450 lb/in. of axial tension. A l-in. long notch was cut into the panel at this critical location to study the damage tolerance characteristics of this sandwich panel concept. The notch was machined into the panel to extend in the panel hoop direction slightly beyond the window frame edge. A combined loading condition with 8.85 psi of internal pressure and 1630 lb/in. of axial load was applied to the panel. This loading condition corresponds to two-thirds of the design ultimate load condition. The panel outer surface hoop and axial strain results from the finite element analysis are presented in Fig. 12 for this combined loading condition. The hoop varies from -1100 μin./in. at $\theta = 90$ deg to 1900 μin./in. at $\theta = 0$ deg. These strain magnitudes are 150% higher than for the hoop strain results presented in Fig. 12 for 13.65 psi of internal pressure and 2450 lb/in. of axial tension. This increase in strain for this test case is due to the increased bending in the skin between the two cutouts caused by the notch. The finite element results for the axial strain at the outer surface along the cutout indicate that the maximum strain of approximately 5200 μin./in. occurs at the tip of the machined notch. The experimental strain results for this load case are presented in Fig. 13a. The test results indicate that the axial strains range from -500 μin./in. to 5800 μin./in. and compare very well with the analysis results. No growth was observed in the notch length during the test. The experimental hoop strain results along the x axis for the three-frame panel, for the two-frame panel, and for the two-frame panel with a notch at the window cutout are compared in Fig. 13b. These results suggest that the far-field strains in the hoop direction are influenced more by the removal of the frame than by the introduction of the notch. The increase in the panel strain state due to the introduction of the notch is local and does not result in any significant load redistribution. These results illustrate that the panel configuration with three and two frames respond in a predictable manner and that the strains are well within the failure strain allowables for this loading condition. The results on the three- and two-frame sandwich side panel suggest that additional structural weight savings are possible when the frame spacing is increased to 40 in.

Combined Axial Compression and Internal Pressure Loading Conditions

Combined Loads Test Machine and D-Box Test Fixture

The combined loads test machine and D-box test fixture configurations are illustrated in Fig. 14. The details of the combined loads test machine are summarized in Ref. 5. The D-box test fixture has been designed to ensure that appropriate boundary conditions are imposed on a curved panel to provide a stress state that is representative of a shell. This requirement is particularly important when the failure of a curved panel is investigated, as well as in damage propagation studies. Analytical studies have been performed on a D-box test fixture with a full-scale stiffened aluminum fuselage panel.

The D-box test fixture shown in Fig. 15a must have adequate radial stiffness to support the pressure load, but have a small axial stiffness compared to the test panel. The small axial stiffness of the D-box test fixture allows a test panel to experience most of the applied axial load and minimizes the shift in the center of pressure of the assembly if the test panel buckles. The low axial stiffness of the D-box test fixture is the result of an assembly of curved I beams with the cross section shown in the inset. The I-beam sections are 8.0 in. deep, and 15 of these sections are used for the D-box test fixture. The axial stiffness of the D-box test fixture is designed to be 5% of a typical curved stiffened panel and D-box test fixture. The axial stiffness of the curved panel is assumed to be 1.1×10^6 lb/in., which is representative of the stiffness of a typical

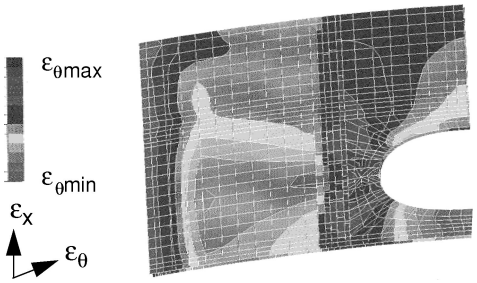

a) Hoop strain

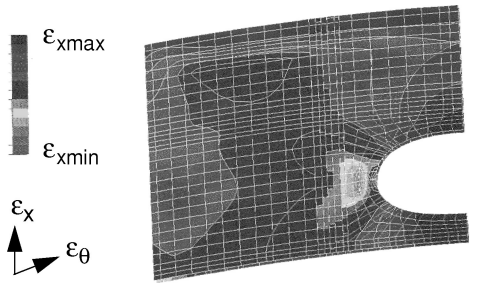

b) Axial strain

Fig. 12 Finite element analysis results for strains on the notched two-frame panel outer surface for a combined 8.85-psi internal pressure and 1630 lb/in. axial loading condition.

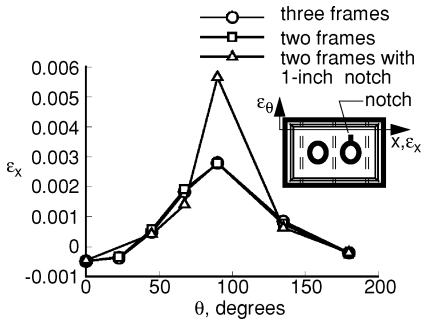

a) Axial strain around cutout

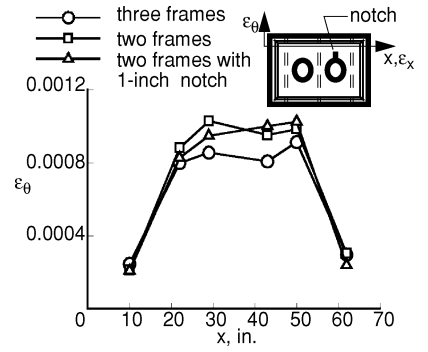

b) Hoop strain

Fig. 13 Comparison of experimental strain results on the three-, two-, and notched two-frame panel outer surface for a combined 8.85-psi internal pressure and 1630 lb/in. axial loading condition.

fuselage shell. This D-box test fixture is designed to test curved panels with 60–130 in. radii and 20–22 in. frame spacings. The panels are attached to the D-box test fixture with the hinge fittings as indicated in Fig. 15b. A cross section of the D-box test fixture is presented in Fig. 15b that shows the details of the hinge fittings. There are 13 of these hinge fittings provided between the I beams for this purpose. When the D-box assembly is internally pressurized, the assembly expands in a manner that causes the hinge supports to move inward. This deformation will cause the test panel to bend in a way that is not representative of the response of an internally pressurized

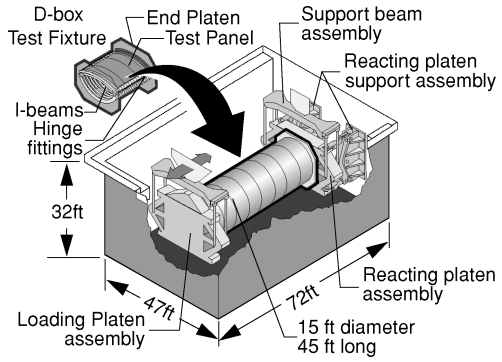

Fig. 14 NASA combined loads test machine.

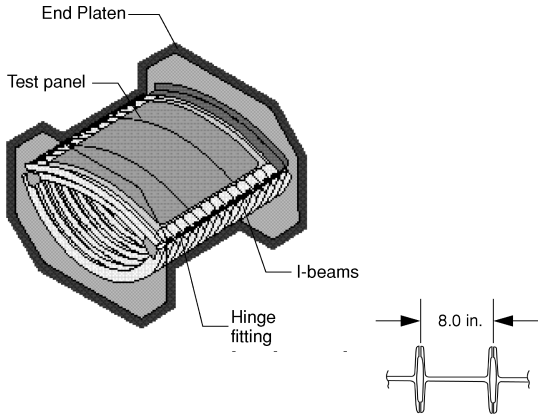

a) Overall configuration

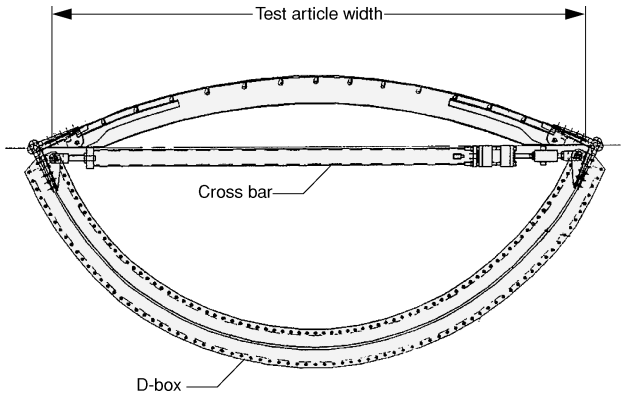

b) Cross-sectional view

Fig. 15 D-box test fixture for testing curved stiffened panels.

shell. To prevent this undesirable deformation, cross bars are mounted between the hinge points, as shown in the Fig. 15b, such that the distance between the hinge points can be held constant or adjusted as needed to induce the appropriate stress state in the test panel.

Description of Finite Element Models

Two important design details significantly influence the stress state in a curved stiffened panel tested in a D-box test fixture. The first design detail is the load introduction region that attaches the curved panel to the D-box test fixture. If the hoop load in the panel from the internal pressure of the D-box assembly is only reacted at the panel boundary by the skin, the panel will be subjected to bending moments at the hinge attachment point. Part of the hinge fitting that attaches the test panel to the D-box test fixture is designed to react to load through the frames, as well as through the skin. The analytical results used to select a hinge fitting design are presented in Ref. 5. The second design detail is the support conditions along the two straight edges of the panel. Appropriate boundary conditions

must be imposed on the panel so that its response compares with the corresponding shell response for a given loading condition. The cross bars have to be designed to apply forces that prevent unwanted radial displacements that would bend the panel at the hinge locations. These design details have been studied by the use of the results of finite element analyses. The finite element models for a cylindrical shell and the D-box test fixture with a corresponding test panel were generated with PATRAN (Ref. 2), and linear and nonlinear structural analyses were performed with NASTRAN (Ref. 6). The nonlinear analyses for the pressure and the combined pressure and axial load cases have been performed for the cylindrical shell case to increase understanding of nonlinear effects.

The shell is modeled with quadrilateral plate elements and has 25,973 degrees of freedom. The D-box test fixture assembly with the curved panel is modeled with plate, bar, beam, and spring elements totaling 6773 elements and 33,130 degrees of freedom. To simulate the cylindrical shell subjected to internal pressure, the curved panel for the D-box test fixture is analyzed with boundary conditions that only permit radial displacements along the straight edge. To simulate the 20-in. long longitudinal crack in the panel, two rows of coincident nodes are generated along the panel centerline, which were disconnected along the 20-in. length.

Curved Panel and Shell Linear Analyses

Finite element analysis results for internal pressure load cases and a combination of internal pressure and axial compression loads are presented herein for both undamaged and damaged curved panels. The entire hoop load developed in a pressurized panel must be supported by the D-box test fixture without the introduction of undesirable boundary effects. When a stiffened curved panel is tested in a D-box test fixture, the test fixture should provide proper support conditions to the panel and induce a stress state that is representative of the corresponding shell structure. Cylindrical shell results are compared with the corresponding curved panel results for internal pressure load cases with and without an axial compression load to study these issues. The panel used for the analytical studies is a full-scale aluminum panel, which will be tested as a proof-test article for the D-box test fixture, which will be loaded in the combined loads test machine. The frame spacing for the panel is 20 in. and the stringer spacing is 6.85 in. The panel is 96 in. wide and 120 in. long, and has a radius of 120 in. A 20-in. long longitudinal crack through the skin and the frame at the midlength is used to represent penetration damage in an aircraft fuselage. The response of the panel with this damage condition will be studied with the panel tests.

Internal Pressure Loads

Two specimen and pressure combinations are considered for the internal pressure load cases. The first combination is the undamaged panel subjected to an 18-psi internal pressure condition that is representative of the burst pressure (ultimate load) condition in a transport aircraft fuselage. The second combination is a panel with 20-in. long penetration damage and subjected to the limit load condition of approximately 9-psi internal pressure. The panel also has a severed frame to simulate penetration damage.

Linear finite element analysis results for the panel in the D-box test fixture subjected to 18 psi of internal pressure, and the results for the corresponding cylindrical shell, are shown in Fig. 16. The resulting hoop stresses in the shell (Fig. 16a) are uniform in the skin and frame regions. The load distribution between the skin and frames is 46 and 54% of the total load, respectively. The maximum hoop stress resultant of 3500 lb/in. occurs on the skin surface opposite to the frame location, and the hoop stress resultants for the inside flange of the frame are 1600 lb/in. The corresponding stress state in the curved panel supported in the D-box test fixture with rigid cross bars to prevent relative displacement between the hinge points is shown in Fig. 16b. The load is not uniformly distributed in the panel skin bays. The load distribution between the frame and the skin are 47 and 53% of the total load, respectively. The load in the middle of the panel has a bending component in addition to the membrane tension component. This undesirable bending moment can be corrected by application of a compressive preload to the cross

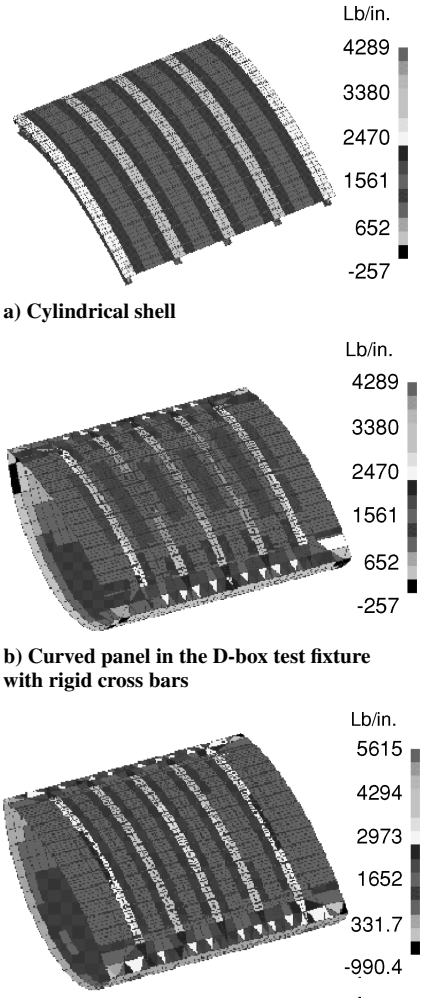

a) Cylindrical shell

b) Curved panel in the D-box test fixture with rigid cross bars

c) Curved panel in the D-box test fixture with preloaded cross bars

Fig. 16 Comparison of hoop stress resultant distributions for the cylindrical shell and the curved stiffened panel for an internal pressure of 18 psi.

bars, which generates in a bending moment in the opposite direction. This correction is accomplished in the analysis by application of a uniform temperature to the cross bars. The cross bars apply an equal and opposite bending moment to the test panel and provide a uniform membrane stress state between the skin bays for a temperature of 150°F. The load distribution between the frames and the skin are also comparable to that of the cylindrical shell case for this 18-psi internal pressure condition, as shown in Fig. 16c.

Analytical results for a panel with a 20-in. long longitudinal crack extending from the center of one skin bay and with a severed frame are shown in Fig. 17. The applied pressure load is 9 psi for this damage condition, which is the design limit pressure for the fuselage. The load distribution for the shell is shown in Fig. 17a and indicates that there is a 25% increase in the stress level in the undamaged frames compared to the undamaged panel results. This loading condition can be simulated in a curved panel in the D-box test fixture. The results of an analysis for this configuration are shown in Fig. 17b.

Combined Internal Pressure and Axial Compression Load Case

Linear analysis has been performed on the shell and the curved panel in the D-box test fixture to determine the loads that need to be applied through the cross bars to simulate the stress state in a shell. The results for the undamaged panel are summarized in Ref. 5. The hoop stress results for a shell with a 20-in. long longitudinal crack and loaded with 2350 lb/in. of axial compression and 9 psig of internal pressure are compared with a corresponding case for the

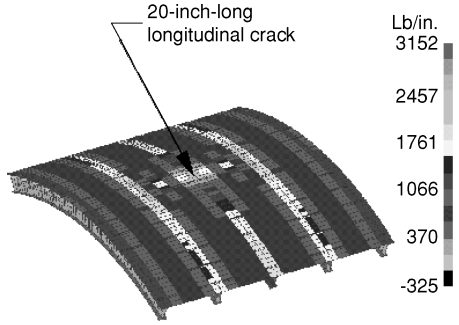

a) Cylindrical shell

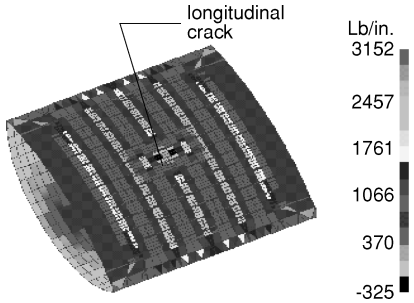

b) Curved panel in the D-box test fixture with loaded cross bars

Fig. 17 Comparison of hoop stress resultants contours for the cylindrical shell with 20-in. long longitudinal crack for 9-psi internal pressure.

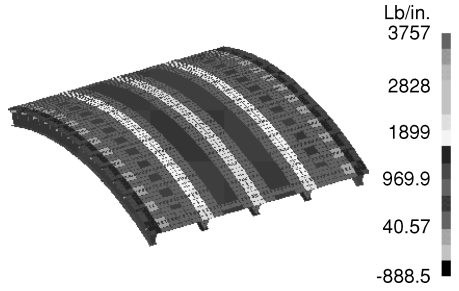

a) Cylindrical shell

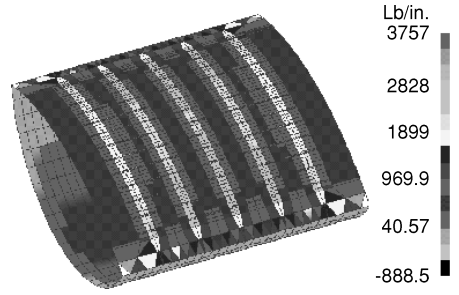

b) Curved panel in the D-box test fixture with loaded cross bars

Fig. 18 Comparison of hoop stress resultant distributions for the cylindrical shell and curved stiffened panel for a combined internal pressure of 9 psi and an axial loading of 2350 lb/in.

damaged curved panel in Fig. 18. The stress resultant distributions for the two surfaces are comparable, as shown in Fig. 18, when the appropriate cross bar forces are applied for this load case. The results indicate that the influence of a 20-in. long longitudinal crack or an axial compression load is approximately the same on the loads in the cross bars. The crossbar forces are minimally affected by the two preceding conditions.

Axial Compression Load Case, Nonlinear Cylindrical Shell Analysis

The proof test of the panel for the combined loads test machine will be loaded in compression to levels beyond buckling. Reductions in curved panel stiffness in the postbuckling load range are determined from a nonlinear analysis to understand the panel response and the associated boundary conditions that must be imposed on the test panel in the D-box test fixture. The internal pressure causes nonuniform skin displacements that cause nonlinear interactions between skin and stringers, and this response must be understood. Shell analyses have been performed for internal pressure and combined pressure and axial loading conditions to help in the understanding of the influence of these nonlinear effects on structural response. A representative shell segment is used for these analyses. The relatively small model size minimizes the computational times associated with the nonlinear analysis. Because the structure will be loaded beyond buckling, the dimensions of this shell segment need to be determined so that the model represents the shell response for compression loads. The cyclic symmetry technique in MSC/NASTRAN (Ref. 6) was used for a linear buckling analysis study to determine the size of this shell segment. The lowest eigenvalue for the shell segment was determined to be for a skin buckling mode with the skin between frames buckling along the shell circumference into 48 half-waves at a total load of 773 lb/in. A shell segment with two stringer spacings was chosen to correspond to this harmonic result. The length of the shell segment was chosen to include three frames to facilitate studies of shell response with a 20-in. long longitudinal crack in the skin and with a failed midframe. Interactions from the boundaries of the shell segment on the internal stress states are expected to be a minimum for this structural size.

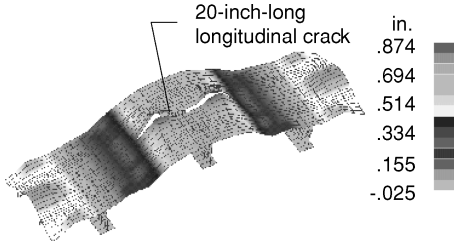

a) Out-of-plane displacement contours

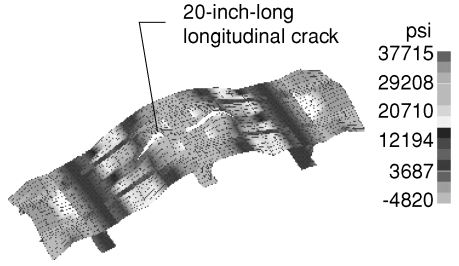

b) Hoop stress contours

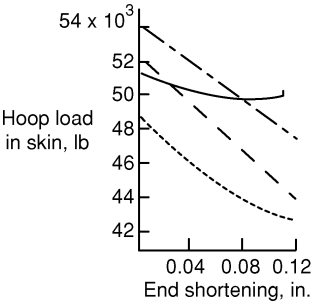

c) Load vs end shortening

Fig. 19 Nonlinear analysis results for the cylindrical shell with 20-in. longitudinal crack for combined 9-psi internal pressure and 1600 lb/in. axial compression loading: - - - -, linear analysis without damage; – – –, nonlinear analysis without damage; – – –, linear analysis with damage; and ——, nonlinear analysis with damage.

The hoop stresses for the damaged shell with the combined load case with 9 psi of internal pressure and 1600 lb/in. of axial compression are presented in Fig. 19. The nonlinear analysis results indicate significantly larger out-of-plane deformations for the damaged shell. The maximum values for the out-of-plane deflection occur in the vicinity of the crack tip. The magnitudes of these deflections are 0.26 and 0.59 in. for the linear and nonlinear analyses, respectively. The maximum hoop stress values for the nonlinear analysis results (Fig. 19b) are twice the values for the linear analysis results. The load distributions between the skin and the frames obtained from nonlinear analysis results for both the undamaged and damaged shell models suggest that the stiffening of the skin due to large deformations enables the skin to support greater loads. The nonlinear analysis results for this axial load condition suggest that the skin supports 50% of the total load in the damaged state compared to 35% for the linear analysis results.

The differences between the load-carrying capability of the skin with and without damage, as obtained from the linear and nonlinear analysis results for the combined pressure and axial load cases are explained by means of Fig. 19c. The change in stiffness of the skin is summarized in Fig. 19c as the end-shortening corresponding to an axial compression load is increased for the pressure loaded panel. Both the linear and nonlinear analysis results suggest that as the compression load is increased, stiffness reduction for the skin in the undamaged state is more than that for the skin in the damaged state. The nonlinear results suggest that, for end-shortening values greater than 0.070 and 0.055 in. for the undamaged and damaged panels, respectively, the skin exhibits a stiffening behavior that results in the skin carrying more load compared to the value obtained from the linear analysis. These analysis results suggest that curved panels subjected to internal pressure and axial compression can be tested in the D-box test fixture to study the response of full-scale shell structures.

Conclusions

A design approach for fuselage shell structures has been summarized that takes performance, producibility, and cost of the structure into consideration during the preliminary design phase. The quality of the preliminary design depends on the accuracy of the structural analysis methods that are available for this part of the design cycle. The approximations and simplifications that are currently being made during this design phase require that experiments be conducted on a full-scale structure to validate the designs. A pressure-box test machine and a D-box test fixture can be used to simulate the shell stress state test panels such that the shell response can be assessed in a relatively inexpensive manner for both undamaged and damaged structures. The comparison of experimental and analytical results reemphasize the importance of the performance of geometrically nonlinear analyses to evaluate the response of thin-walled structures subjected to combined mechanical and pressure loading conditions.

References

[1]Rouse, M., and Ambur, D. R., "Fuselage Response Simulation of Stiffened Panels Using a Pressure-Box Test Machine," AIAA-95-1362-CP, April 1995.

[2]Anonymous, "PATRAN Plus User Manual—Release 2.4," PDA Engineering, Los Angeles, Publication Number 2191023, Sept. 1989.

[3]Brogan, F. A., Rankin, C. C., and Cabiness, H. D., "STAGS User Manual," Lockheed Martin Missiles and Space Company, Palo Alto Research Lab., Palo Alto, CA, Rept. LMSC P032594, 1994.

[4]Anonymous, "ABAQUS Finite Element Code," Hibbit, Karlsson, and Sorensen, Inc., Pawtucket, RI, Vol. 1–2, 1995.

[5]Ambur, D. R., Cerro, J. A., and Dickson, J. N., "Analysis of a D-Box Fixture for Testing Stiffened Panels in Compression and Pressure," *Journal of Aircraft*, Vol. 32, No. 6, 1995, pp. 1382–1389.

[6]Anonymous, "MSC/NASTRAN Handbook for Linear Analysis—Version 64," MacNeal–Schwendler Corp., Los Angeles, Aug. 1985.